

## Extensive Pancreas Regeneration Following Acinar-Specific Disruption of Xbp1 in Mice

DAVID A. HESS,\* SEAN E. HUMPHREY,\* JEFF ISHIBASHI,\* BARBARA DAMSZ,\* ANN-HWEE LEE,†  
LAURIE H. GLIMCHER,‡ and STEPHEN F. KONIECZNY\*

\*Department of Biological Sciences and the Purdue Center for Cancer Research, Purdue University, West Lafayette, Indiana; and †Department of Immunology and Infectious Diseases, Harvard School of Public Health, and Department of Medicine, Harvard Medical School, Boston, Massachusetts

See editorial on page 1155.

**BACKGROUND & AIMS:** Progression of diseases of the exocrine pancreas, which include pancreatitis and cancer, is associated with increased levels of cell stress. Pancreatic acinar cells are involved in development of these diseases and, because of their high level of protein output, they require an efficient, unfolded protein response (UPR) that mediates recovery from endoplasmic reticulum (ER) stress following the accumulation of misfolded proteins. **METHODS:** To study recovery from ER stress in the exocrine organ, we generated mice with conditional disruption of Xbp1 (a principal component of the UPR) in most adult pancreatic acinar cells (Xbp1<sup>fl/fl</sup>). We monitored the effects of constitutive ER stress in the exocrine pancreas of these mice. **RESULTS:** Xbp1-null acinar cells underwent extensive apoptosis, followed by a rapid phase of recovery in the pancreas that included expansion of the centroacinar cell compartment, formation of tubular complexes that contained Hes1- and Sox9-expressing cells, and regeneration of acinar cells that expressed Mist1 from the residual, surviving Xbp1+ cell population. **CONCLUSIONS: XBP1 is required for homeostasis of acinar cells in mice; ER stress induces a regenerative response in the pancreas that involves acinar and centroacinar cells, providing the needed capacity for organ recovery from exocrine pancreas disease.**

*Keywords:* Endoplasmic Reticulum Stress; Pancreatic Progenitor Cells; Protein Folding; Tissue Regeneration.

The pancreas is a complex secretory organ tasked with endocrine-mediated maintenance of blood glucose levels and exocrine production of key enzymatic components of the digestive system. Defects or damage to various pancreatic cells contribute to multiple disease states, including diabetes, pancreatitis, and pancreatic cancer, the latter two being diseases associated with the exocrine pancreas. An understanding of the response of pancreatic tissues to damage and stress is of great interest as a means of exploring the development of disease and as a potential avenue for therapeutic intervention.

As professional secretory cells, pancreatic acinar cells are responsible for the synthesis, storage, and secretion of vast quantities of digestive hydrolases that assist in food digestion.<sup>1</sup> One of the key requirements for the proper function

and survival of acinar cells is the management of their extensive protein synthesis/processing machinery, which uses regulatory pathways involving the Golgi, intermediate transport vesicles, plasma membrane components, and the endoplasmic reticulum (ER). Among these organelles, the ER ensures that newly synthesized secretory and transmembrane proteins are properly folded and modified before exportation. In cells with high protein synthesis demands,<sup>2,3</sup> with specific differentiation requirements,<sup>2,4,5</sup> or that are subject to environmental or physiologic alterations, the ability of the protein-folding machinery to handle the synthetic load can reach an imbalance, setting in motion a series of intracellular signaling pathways collectively known as the unfolded protein response (UPR).<sup>6-8</sup> Activation of the UPR allows cells to adjust to high protein demands by transcriptionally activating genes that increase protein-folding capacity.

The UPR consists of 3 distinct signaling arms (inositol-requiring transmembrane kinase/endonuclease 1 [IRE1]/X-box binding protein 1 [XBP1], activating transcription factor 6 [ATF6], and protein kinase RNA-like ER kinase [PERK]), each of which activates unique downstream target genes and pathways (eg, XBP1-protein disulfide isomerase [PDI], subunit of the Sec61 transport protein complex [Sec61a]; ATF6-nATF6 $\alpha$ ; PERK-p-eIF2 $\alpha$ ).<sup>8</sup> The ER inositol-requiring transmembrane kinase/endonuclease 1 (IRE1) branch activates multiple classes of molecules, including chaperones (PDI), protein transporters (Sec61a), and growth/DNA damage regulators (GADD153-C/EBP-homologous protein [CHOP]). IRE1 oligomerizes and autophosphorylates in response to unfolded proteins in the ER lumen, resulting in activation of its novel endoribonuclease domain. Activated IRE1 excises a 26-nucleotide fragment within the basal Xbp1 transcript, producing a frame shift and consequent translation of a 371-amino

*Abbreviations used in this paper:* ATF6, activating transcription factor 6;  $\beta$ -gal,  $\beta$ -galactosidase; CHOP, C/EBP-homologous protein; CPA, carboxypeptidase; ER, endoplasmic reticulum; IRE1, inositol-requiring transmembrane kinase/endonuclease 1; PERK, protein kinase RNA-like ER kinase; PDI, protein disulfide isomerase; Sec61a, subunit of the Sec61 transport protein complex; TM, tamoxifen; TUNEL, terminal deoxynucleotidyl transferase-mediated deoxyuridine triphosphate nick-end labeling; UPR, unfolded protein response; Xbp1, X-box binding protein 1; Xbp1s, Xbp1 spliced version; ZC, zymogenic cell; ZG, zymogen granule.

© 2011 by the AGA Institute

0016-5085/\$36.00

doi:10.1053/j.gastro.2011.06.045

acid XBP1s (“spliced”) transcription factor that functions to up-regulate UPR target genes.<sup>2,8</sup>

The high protein synthesis capacity of pancreatic acinar cells suggests that they likely rely on an efficient IRE1/XBP1 pathway to maintain proper protein processing.<sup>9</sup> In support of this idea, Iwawaki et al have shown that the IRE1/XBP1 pathway is constitutively active in the exocrine pancreas.<sup>10,11</sup> Similarly, acinar cells undergoing acute pancreatitis exhibit elevated levels of ER stress accompanied by activation of the Xbp1 splicing machinery.<sup>6,7,10</sup> Indeed, embryonic deletion in *Xbp1*<sup>-/-</sup>; *Liv*<sup>XBP1</sup> mice results in pancreata that are severely devoid of acinar cells, leading to neonatal death due to limited food digestion and consequent hypoglycemia.<sup>3</sup> XBP1 is also essential for plasma cell differentiation<sup>2</sup> and is critical for tumor angiogenesis in pancreatic adenocarcinoma,<sup>11</sup> revealing a central role for this factor in many different biologic contexts. Because XBP1 possesses additional functions in normal cell development<sup>2,4,12</sup> outside ER stress maintenance, it has been difficult to assess the importance of the IRE1/XBP1 pathway in the adult exocrine pancreas. To circumvent this obstacle, we conditionally inactivated an *Xbp1*<sup>fl/fl</sup> allele in adult acinar cells to address 2 key questions: (1) What is the fate of individual acinar cells undergoing chronic ER stress in the absence of the IRE1/XBP1 pathway? and (2) How does the exocrine organ cope with defective secretory cells? Our results show that loss of XBP1 function is lethal to mature acinar cells. However, the pancreas itself exhibits a remarkable ability to recover from chronic ER stress by eliciting a rapid regeneration response from a minority of unrecombined *Xbp1*<sup>fl/fl</sup> acinar cells as well as from *Hes1*/*Sox9*-positive centroacinar progenitor cells. We conclude that the IRE1/XBP1 pathway is critical to maintaining normal ER homeostasis and that exploiting ER stress represents a novel approach to generating and studying pancreatic damage in vivo.

## Materials and Methods

### Mouse Strains and Genotyping

*Mist1*<sup>CreER/+</sup> and *Xbp1*<sup>fl/fl</sup> mice have been described previously.<sup>4,13,14</sup> Induction of Cre-ER<sup>T2</sup> activity was accomplished by providing adult mice (6–8 weeks old) with tamoxifen (TM; 4 mg/mouse/day) for 2 consecutive days. Mice were sacrificed at 1-week intervals after addition of tamoxifen, and pancreata were harvested using standard protocols. Genotyping and recombination primer sets are listed in Supplementary Table 1. All studies were conducted in compliance with National Institutes of Health and the Purdue University Institutional Animal Care and Use Committee guidelines.

### Histology and Immunohistochemistry

Mouse pancreata were fixed in 10% neutral buffered formalin, paraffin embedded, sectioned to 5 μM, and stained using conventional H&E. Sections were deparaffinized and retrieved using the 2100 Retriever (PickCell Laboratories, Amsterdam, The Netherlands) and antigen unmasking solution (Vector Laboratories, Burlingame, CA). Samples were blocked using the MOM blocking reagent (Vector Laboratories), and incubation of primary antibodies was conducted overnight at 4°C. Biotinyl-

ated secondary antibodies were applied for 10 minutes at 25°C. Visualization was accomplished via 3,3'-diaminobenzidine tetrahydrochloride peroxidase staining (Vector Laboratories) or tertiary, avidin-conjugated fluorescent antibodies. Primary antibodies and conditions are provided in Supplementary Table 2. Terminal deoxynucleotidyl transferase-mediated deoxyuridine triphosphate nick-end labeling (TUNEL) assays were performed following digestion in 250 μg/mL proteinase K in 2.5 mmol/L CaCl<sub>2</sub>, 10 mmol/L Tris-HCl, pH 7.5, for 1 minute at 25°C using the In Situ Death Detection Kit (Roche, Indianapolis, IN).

### Electron Microscopy

Pancreata were fragmented and fixed in 3% paraformaldehyde/0.5% glutaraldehyde in phosphate-buffered saline and then gradually dehydrated and embedded in Epon resin (EMS, Hatfield, PA). Electron micrographs were obtained from ultrathin sections using a Philips transmission electron microscope (Philips, Andover, MA).

### Protein Immunoblot Assays

Twenty micrograms of whole cell protein extracts were separated on 12% acrylamide gels, transferred to polyvinylidene difluoride membranes, and incubated with primary antibodies (antibody conditions are provided in Supplementary Table 3). Immunoblots were developed using an enhanced chemiluminescence kit (Pierce, Rockford, IL).

### Reverse-Transcription Quantitative Polymerase Chain Reaction Gene Expression Analysis

Pancreas RNA was isolated using the RNeasy Isolation System (Qiagen, Valencia, CA) and reverse transcribed using the iScript cDNA Synthesis Kit (Bio-Rad, Hercules, CA). Complementary DNA reactions were amplified with QPCR SYBR Green Mix (Abgene, Epsom, United Kingdom) as described in Supplementary Materials and Methods using the primer sets listed in Supplementary Table 4.

## Results

### Acinar-Restricted Deletion of *Xbp1*

To examine the importance of XBP1 and the UPR pathway to the mature exocrine pancreas, we used conditional null *Xbp1*<sup>fl/fl</sup> mice<sup>4</sup> crossed to *Mist1*<sup>CreER/+</sup> mice, which express CreER<sup>T2</sup> exclusively in acinar cells<sup>13,14</sup> (Figure 1A). Control pancreata from vehicle-treated adult *Xbp1*<sup>fl/fl</sup>; *Mist1*<sup>CreER/+</sup> mice showed no signs of Cre-mediated recombination and were phenotypically indistinguishable from pancreata obtained from wild-type, *Xbp1*<sup>fl/fl</sup>, or *Mist1*<sup>CreER/+</sup> animals (Figure 1B and Supplementary Figure 1). In contrast, tamoxifen (TM)-treated *Xbp1*<sup>fl/fl</sup>; *Mist1*<sup>CreER/+</sup> mice exhibited pancreas-restricted recombination that deleted exon 2 from the *Xbp1* locus (Figure 1B). As predicted, administration of TM also led to pancreas-specific expression of *Xbp1*<sup>ΔEx2</sup> transcripts within 24 hours (Figure 1C). Lineage tracing using *Xbp1*<sup>fl/fl</sup>; *Mist1*<sup>CreER/+</sup>; *R26*<sup>LacZ</sup> mice revealed no recombination in the absence of TM but robust recombination (β-galactosidase [β-gal] positive, blue) in approximately 90% of acinar cells (Figure 1D and E).

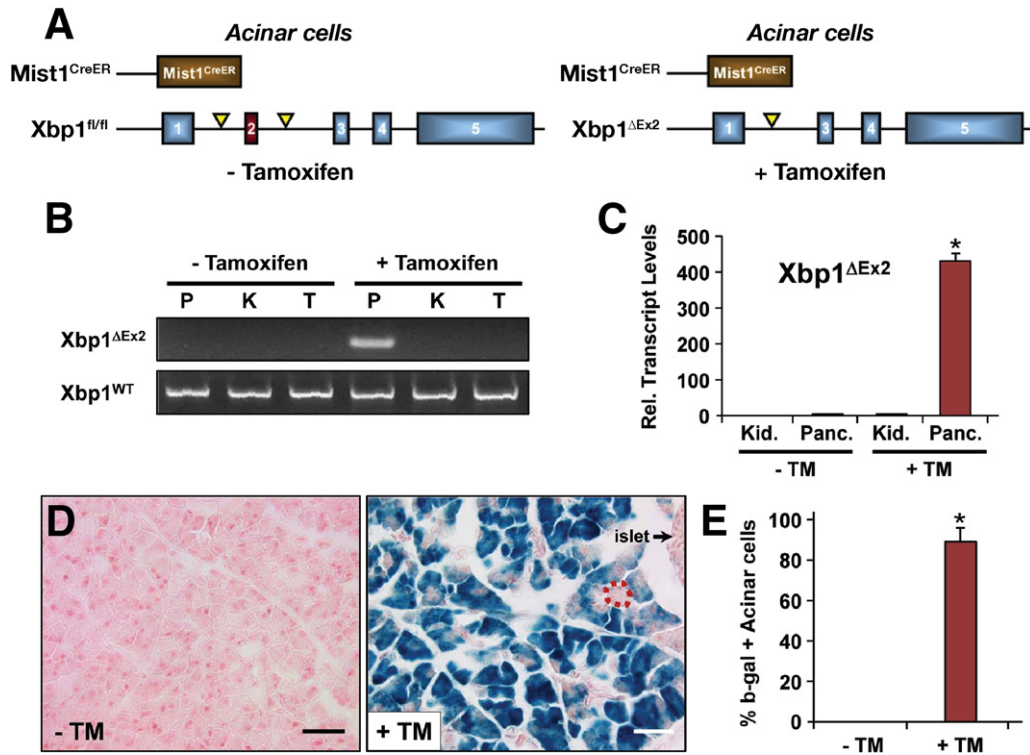


**Figure 1.** Xbp1<sup>fl/fl</sup>;Mist1<sup>CreER/+</sup> mice selectively ablate Xbp1 in pancreatic acinar cells. (A) Schematic representation of the Xbp1<sup>fl/fl</sup> and Xbp1<sup>ΔEx2</sup> alleles from untreated and TM-treated mice. (B) Xbp1<sup>ΔEx2</sup>-specific polymerase chain reaction reveals pancreas-restricted excision of exon 2 following treatment with TM (P, pancreas; K, kidney; T, tail DNA). (C) Transcript analysis of the recombined Xbp1<sup>ΔEx2</sup> locus confirms Xbp1<sup>ΔEx2</sup> transcripts exclusively in pancreatic samples after treatment with TM (Kid., kidney; Panc., pancreas RNA). (D) Representative fields of Xbp1<sup>fl/fl</sup>;Mist1<sup>CreER/+</sup>; R26R<sup>LacZ</sup> pancreata treated with or without TM and stained for β-gal. Dotted red outline shows a rare β-gal-negative acinus. Scale bar = 40 μm. (E) Quantification of β-gal-positive acinar cells in Xbp1<sup>fl/fl</sup>;Mist1<sup>CreER/+</sup>;R26R pancreata. \*P < .005.

To establish the importance of XBP1 to adult acinar cell homeostasis, we next analyzed individual Xbp1<sup>fl/fl</sup>; Mist1<sup>CreER/+</sup> (+TM) animals (hereafter named Xbp1<sup>ΔEx2</sup>) over an extended time course. As expected, mice heterozygous for Xbp1 (Xbp1<sup>ΔEx2/+</sup>) exhibited no signs of ER stress (Supplementary Figure 1). In contrast, Xbp1<sup>ΔEx2</sup> pancreata showed large increases in the general ER stress pathway components Bip and Chop as well as within the PERK and ATF6 arms of the UPR, as indicated by increased levels of phospho-eIF2α and nuclear ATF6α, the immediate effectors of PERK and ATF6, respectively (Figure 2A) (see Supplementary Table 5 for a list of individual molecular markers used in this study). Similarly, the XBP1 arm of the UPR exhibited elevated expression of Xbp1s transcripts over this period (Figure 2B). However, because Xbp1<sup>ΔEx2</sup> transcripts generate a nonfunctional protein,<sup>4</sup> normal XBP1 downstream target genes including Sec61a and PDI were not significantly induced (Figure 2B). Examination of acinar cell differentiation markers revealed a 60% to 70% reduction in amylase and elastase levels over the duration of the study (Figure 2C and D). Likewise, the 37-kilodalton cleaved, active form of carboxypeptidase A (CPA<sup>Active</sup>) was readily detected in Xbp1<sup>ΔEx2</sup> pancreata, reflecting an induced damage response because pancreas CPA is normally stored as an inactive proenzyme except in cases of injury (Figure 2D).<sup>15</sup> Therefore, loss of Xbp1 results in significant alterations in acinar cell properties despite activation of the remnant UPR pathways.

Even with large changes in the expression profiles of UPR pathway components and acinar cell differentiation genes, Xbp1<sup>ΔEx2</sup> pancreata at 24 hours or 1 week after treatment with TM had no significant gross morphology deficiencies. Early time point Xbp1<sup>ΔEx2</sup> acinar cells exhibited the typical accumulation of zymogen granules (ZGs) and normal apical-basal organization of functional acini (Figure 3A). However, by 2 weeks after treatment with TM, Xbp1<sup>ΔEx2</sup> pancreata showed substantial alterations in acinar cell structure, with a reduction in ZGs and loss of cytoplasmic area (Figure 3B). At 4 weeks, Xbp1<sup>ΔEx2</sup> pancreata were severely compromised. Ducts and islets were grossly normal (Supplementary Figure 2), while the vast majority of acinar cells were defective, showing a complete loss of ZG accumulation and a greatly reduced cytoplasmic footprint (Figure 3C). These changes were vividly illustrated by transmission electron microscopy. Low-magnification examination of toluidine-stained semithin sections from 4-week post-TM samples revealed extensive disruption of the exocrine pancreas where the vast majority of acinar cells had greatly reduced cytoplasm and only rare ZGs (Figure 3D). The few ZGs in Xbp1<sup>ΔEx2</sup> acinar cells were small and lacked electron-dense material or were found within autophagic complexes (Figure 3E and F and Supplementary Figure 3). Analysis of ER architecture revealed a poorly developed and dilated ER with disorganized cisternae within Xbp1<sup>ΔEx2</sup> acinar cells. This was in contrast to the elaborately organized and densely packed ER found in con-

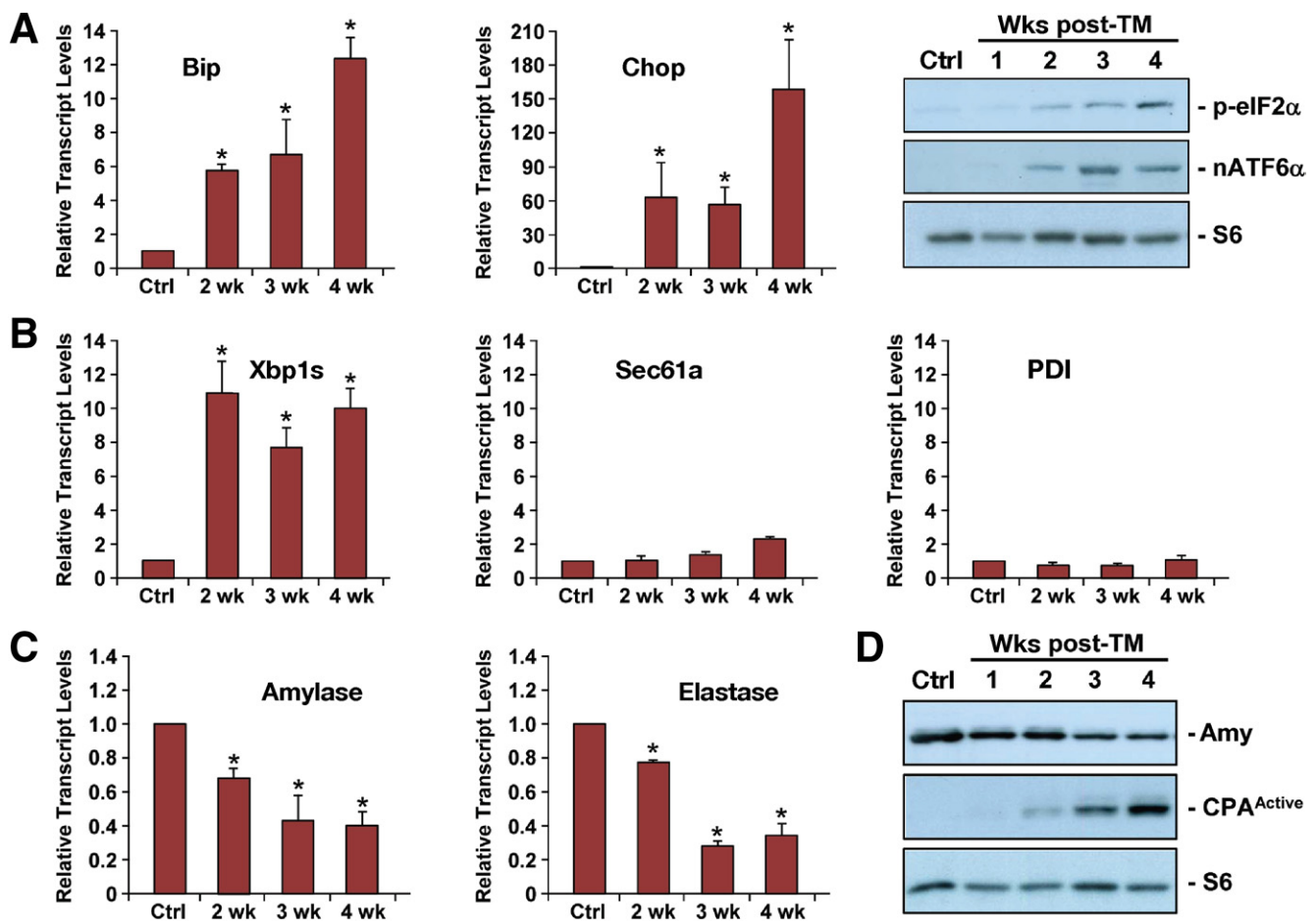


**Figure 2.** Activation of the UPR following acinar-specific ablation of Xbp1. (A) Relative transcript or protein levels of common ER stress indicators, including BiP, Chop, phospho-eIF2 $\alpha$ , and nuclear ATF6 $\alpha$  and (B) Xbp1s following ablation of Xbp1 over the indicated post-TM time points. (B) Xbp1-specific targets Sec61a and PDI do not exhibit increased expression following Xbp1 ablation. (C) Relative transcript levels of amylase and elastase are decreased following Xbp1 ablation. (D) Protein blots revealing decreased production of amylase and increased production of the cleaved, active form of carboxypeptidase (CPA<sup>Active</sup>), an indicator of intracellular damage to acinar cells. S6, loading control; ctrl, littermate animals treated with corn oil. \* $P < .05$ .

control acinar cells. Whereas the majority of ribosomes in control pancreata were ER associated, Xbp1 <sup>$\Delta$ Ex2</sup> acinar cells were filled with abundant free ribosomes that were not part of the defective ER (Figure 3E and F and Supplementary Figure 3). Taken together, these results show that, in the absence of functional XBP1 protein, the exocrine pancreas undergoes a sustained period of ER stress.

### *Xbp1 <sup>$\Delta$ Ex2</sup> Pancreata Exhibit 2 Distinct Acinar Cell Populations*

Although most of the Xbp1 <sup>$\Delta$ Ex2</sup> exocrine pancreas consisted of a nonzymogenic acinar cell population 4 weeks after recombination of the Xbp1<sup>fl/fl</sup> locus, small isolated clusters of relatively normal (zymogenic) acinar cells remained within the organ (Figure 3C and D). These cells retained a typical acinus structure and contained large numbers of ZGs, suggesting that they represented the ~10% of acinar cells that failed to undergo Cre-mediated recombination of the Xbp1<sup>fl/fl</sup> locus (see Figure 1D and E). Indeed, lineage tracing on 4-week Xbp1 <sup>$\Delta$ Ex2</sup>; R26<sup>LacZ</sup> mice revealed that the nonzymogenic acinar cell

population was almost entirely  $\beta$ -gal positive, identifying those cells as Xbp1 <sup>$\Delta$ Ex2</sup> cells (Figure 4A and Supplementary Figure 4). In contrast, isolated groups of intact, zymogenic-acinar cells remained mostly  $\beta$ -gal negative, although rare (~1%)  $\beta$ -gal-positive zymogenic cells (ZCs) were observed, presumably reflecting cells that successfully recombined the R26<sup>LacZ</sup> locus but not both Xbp1<sup>fl/fl</sup> alleles. As predicted, the  $\beta$ -gal-negative acinar cell units maintained high levels of amylase expression (Figure 4B). The ZCs also expressed nuclear MIST1 protein (Figure 4B), which is required to maintain key acinar cell properties.<sup>15</sup> Xbp1 <sup>$\Delta$ Ex2</sup> pancreata exhibited a 3.5-fold increase in overall Mist1 transcript levels despite having only ~10% of cells expressing MIST1 protein (Figure 4C). In contrast,  $\beta$ -gal-positive, non-ZCs barely retained detectable levels of acinar cell markers (Figure 4B). The non-ZCs also had elevated levels of specific ER stress pathway components; for instance, 98% of all CHOP-positive cells were non-ZCs (Figure 4D). Cells expressing CHOP were also prone to apoptosis, because TUNEL staining revealed a dramatic increase in the number of apoptotic cells over the 4-week

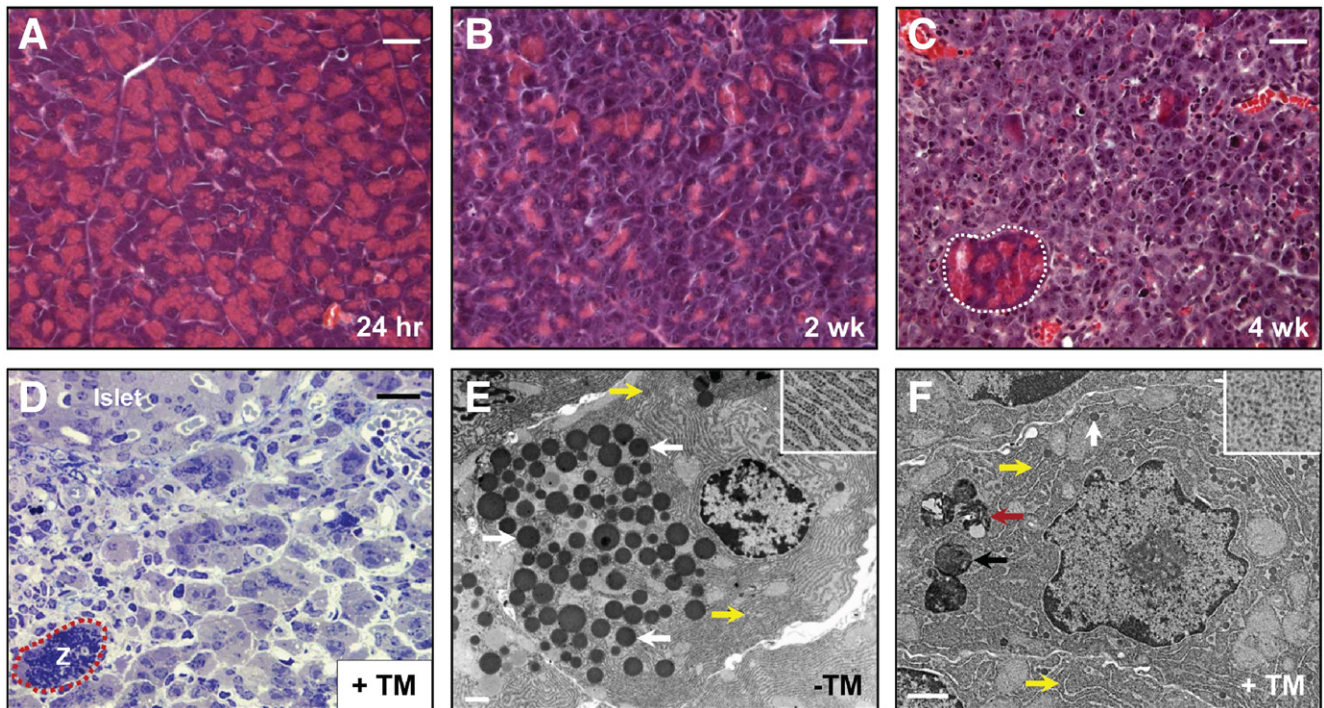


**Figure 3.** Ablation of Xbp1 leads to severe loss of ZGs and alterations in ultrastructure. (A) H&E staining of pancreata 24 hours following Xbp1 ablation. No difference is seen when compared with wild-type pancreata. (B) Pancreas 2 weeks after Xbp1 ablation. Reduction in eosinic staining across the pancreas is visible, suggesting significant alterations to the ZG compartment. (C) Pancreas 4 weeks after Xbp1 ablation. More than 90% of the exocrine pancreas displays little to no eosinic staining. Rare, isolated regions of acinar-like, ZG-bearing cells remain (white outline). (D) Toluidine blue staining of semi-thin sections reveals a completely disrupted exocrine pancreas 4 weeks after treatment with TM. Note the rare zymogenic (z) acinar area (red outline) that remains at this time point. (E) Electron micrograph of a control Xbp1<sup>fl/fl</sup>; Mist1<sup>CreER/+</sup> acinar cell. The extensive accumulation of normal ZGs (white arrows) is apically localized. Highly organized rER (yellow arrows and inset) are also visible at the basal edge of the cell. (F) Electron micrograph of a typical nonzymogenic acinar cell from 4 weeks after TM-treated Xbp1<sup>fl/fl</sup>; Mist1<sup>CreER/+</sup> mice. Autolysosomes (red arrow), autophagosomes (black arrow), disorganized ER (yellow arrows), and small, abortive ZGs (white arrow) can be seen. Inset shows a high-magnification image of the extensive free ribosomes found in these cells. Scale bars: A–D, 30  $\mu$ m; E and F, 1  $\mu$ m.

post-TM period with the majority (96%) found within the nonzymogenic,  $\beta$ -gal-positive cell population (Figure 4D). These cells also exhibited autophagy and activation of other stress pathway components, including elevated levels of pErk1/2 and p38 as part of their terminal end point response to loss of XBP1 (Supplementary Figure 5), confirming a critical role for XBP1 in controlling cellular homeostasis.

The extensive tissue damage that occurred over the 4-week post-TM period in Xbp1 <sup>$\Delta$ Ex2</sup> pancreata prompted us to ask if the organ responded to loss of XBP1 by activating transcription programs associated with pancreatic progenitor cells during embryonic development or pancreatic injury. Previous studies have shown that pancreatic progenitor cells increase expression of a number of genes including Nestin and the transcription factors Hes1 and Sox9, proteins normally restricted to centroacinar cells.<sup>16–19</sup> Each of these genes is up-regulated in the Xbp1 <sup>$\Delta$ Ex2</sup> model, with maximum expression detected at 4 weeks (Figure 4E). Expression of both proteins was restricted to centroacinar/terminal duct cells in the Xbp1 <sup>$\Delta$ Ex2</sup> pancreata (Figure 4F). Zymogenic cells and non-ZCs remained Hes1/Sox9 negative. Thus, extensive Xbp1 <sup>$\Delta$ Ex2</sup>-induced apoptosis leads to a massive damage response within the exocrine pancreas that includes activation of putative Hes1/Sox9 pancreas progenitor cells.

### ***Xbp1 <sup>$\Delta$ Ex2</sup> Pancreata Initiate a Potent Regeneration Response to Replace the Acinar Cell Compartment***

Although approximately 90% of the Xbp1 <sup>$\Delta$ Ex2</sup> exocrine pancreas was severely disrupted in 4-week post-TM mice (see Figure 3C and D), dramatic changes in pancreas gene expression patterns occurred over the ensuing 2 weeks. Expression of downstream ER stress pathway genes, including Bip, Chop, p-eIF2 $\alpha$ , nATGF6 $\alpha$ , and Xbp1u $\rightarrow$ Xbp1s splicing, quickly returned to control basal levels by 6 weeks after treatment with TM (Figure 5A). Similarly, Nestin, Hes1, and Sox9 transcripts peaked at 4 weeks after treatment with TM and then returned to near control levels by 6 weeks (Figure 5B). Changes in differentiation genes were also observed, with Mist1 transcripts peaking at 4 weeks after treatment with TM but gradually returning to control levels by 6 weeks (Figure 5C). The decreases in Mist1, Nestin, Hes1, and Sox9 transcripts correlated with a resurgence in amylase and elastase transcripts and disappearance of cleaved (active) CPA, such that expression of zymogen hydrolases returned to control levels by 6 weeks after treatment with TM (Figure 5D and E).

The complete restoration of molecular markers to control levels after 6 weeks suggested that the apoptotic Xbp1 <sup>$\Delta$ Ex2</sup> acinar cells were replaced, possibly from the

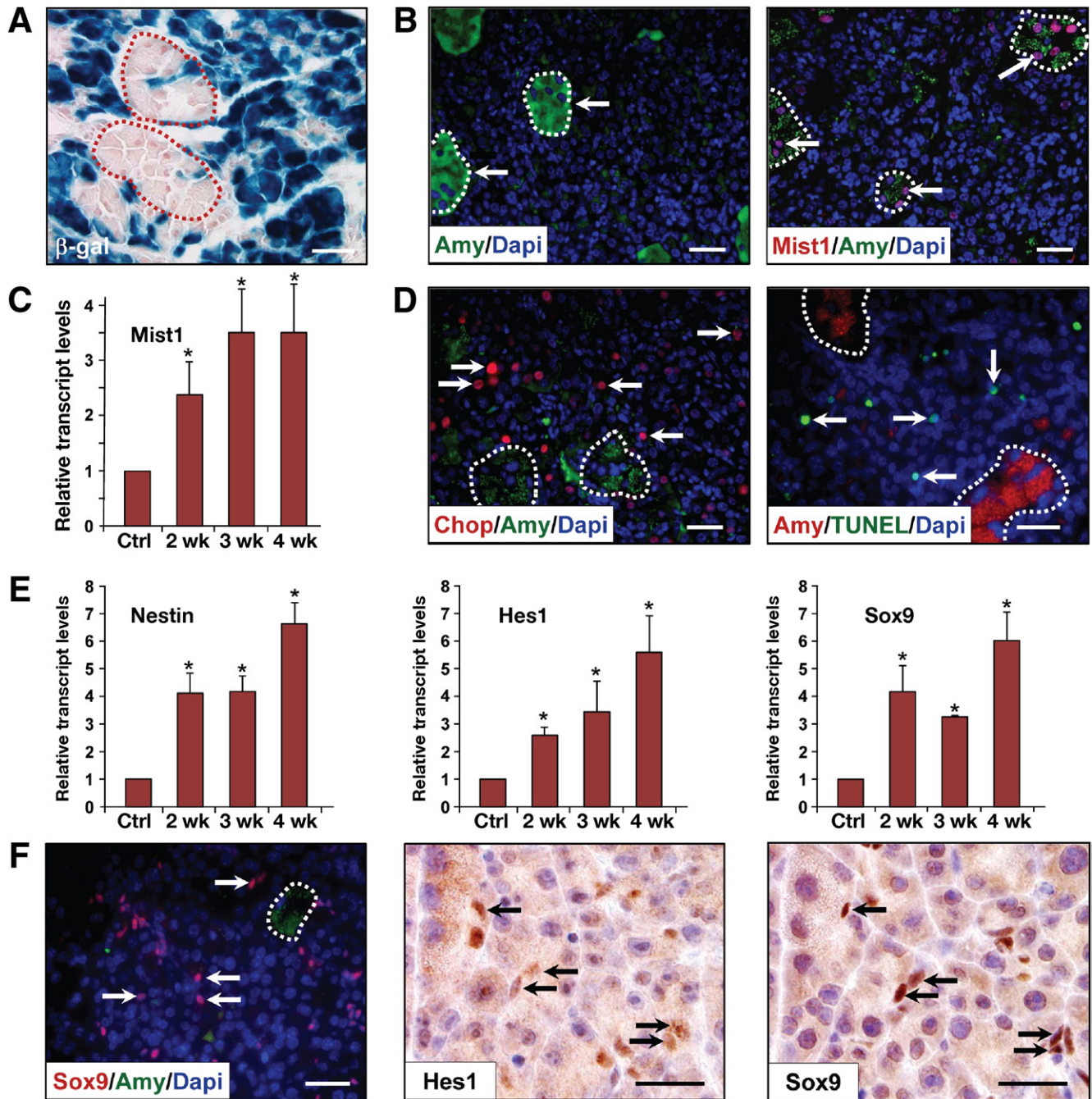


**Figure 4.**  $Xbp1^{\Delta Ex2}$  acinar cells extinguish acinar-specific gene expression and undergo ER stress and programmed cell death. (A)  $\beta$ -gal expression in  $Xbp1^{fl/fl};Mist1^{CreER/+};R26^{LacZ}$  pancreata 4 weeks after treatment with TM. The majority of acinar cells are nonzymogenic  $\beta$ -gal positive, although isolated, zymogen-containing clusters of acinar cells (outlines) remain  $\beta$ -gal negative. (B) Zymogen-containing regions (arrows) accumulate high levels of amylase and MIST1, a transcription factor linked to terminal differentiation of the exocrine pancreas. (C) Relative transcript levels of *Mist1* reveal an increase in expression following *Xbp1* ablation despite restriction to only the ZC population. (D) Localization of the ER stress indicator CHOP and TUNEL-positive cells (arrows) is largely restricted to non-ZCs. Dotted outlines indicate individual zymogen-containing acinar units. (E) Relative transcript levels of pancreatic progenitor cell genes *Nestin*, *Hes1*, and *Sox9* following *Xbp1* ablation. (F) Expansion of the centroacinar/terminal duct cell compartment is detected by increased numbers of *Hes1*- and *Sox9*-positive cells (arrows), which are amylase negative. Bright-field immunohistochemistry *Hes1*, *Sox9*: serial sections. Scale bars = 20  $\mu$ m. \* $P < .05$ .

small subset that escaped TM-induced recombination. By 4 weeks after treatment with TM, the remaining  $Xbp1^{fl/fl}$  ZCs were generally present as individual acinus units scattered among the apoptotic, nonzymogenic population. These  $\beta$ -gal-negative cells showed a dramatic increase in cell proliferation that peaked at 3–4 weeks after treatment with TM (Figure 6A and Supplementary Figure 6).

Indeed, more than 80% of all proliferating cells at this time point were zymogenic acinar cells, with the remaining proliferative cells mostly *Sox9*-positive centroacinar/terminal duct cells (Figure 6B). Additionally, the regeneration response also included transient up-regulation of the *Reg1* gene (Supplementary Figure 6). As predicted, despite extensive  $\beta$ -gal expression from the  $R26^{LacZ}$  locus

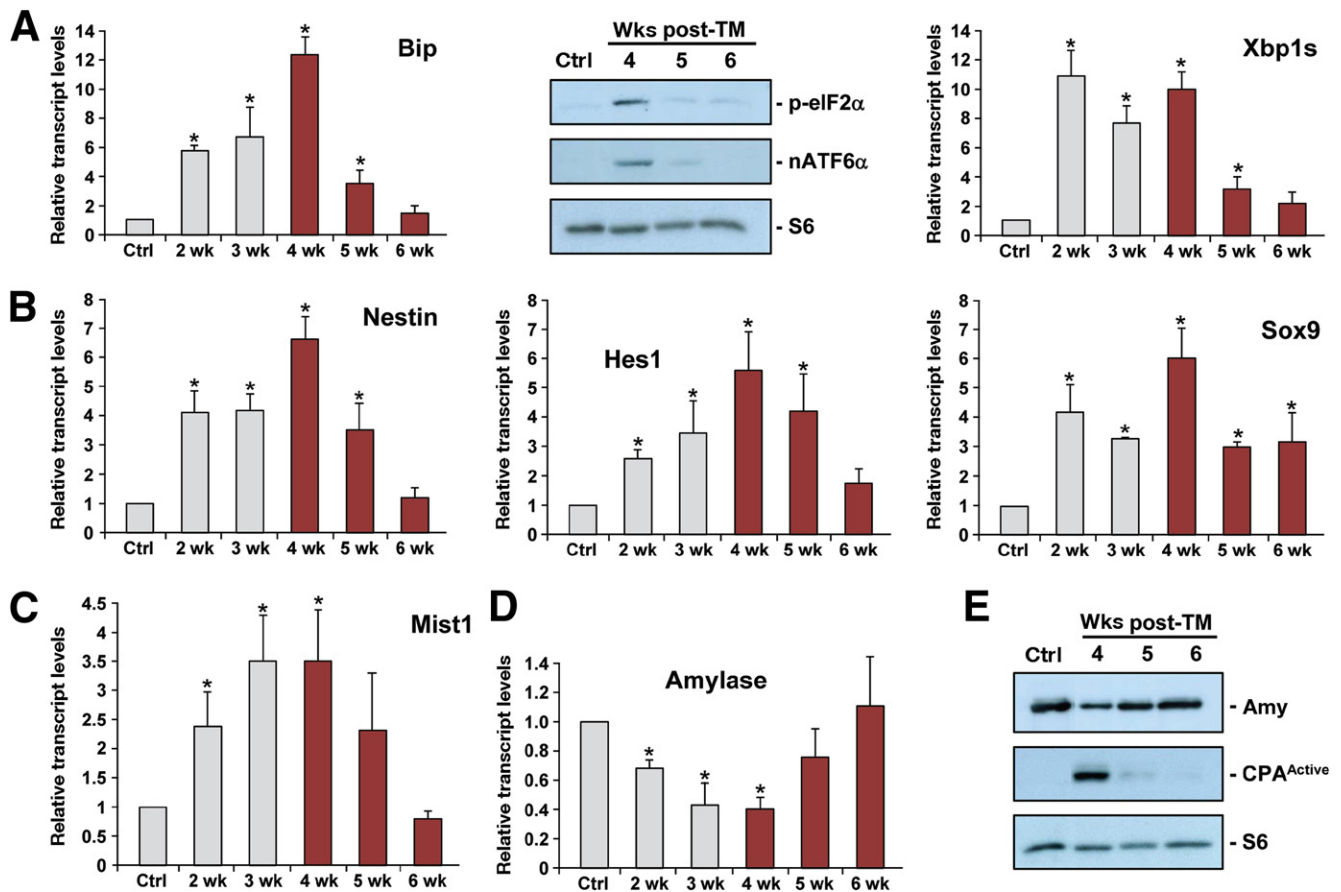


**Figure 5.** Xbp1<sup>ΔEx2</sup> pancreata undergo a rapid recovery period following peak ER stress and apoptosis responses. (A) Relative transcript and protein levels of the ER stress markers BiP, p-eIF2 $\alpha$ , nATF6 $\alpha$ , and Xbp1s are reduced to near control levels over the 4- to 6-week post-TM period. (B) Relative transcript levels of pancreatic progenitor cell genes Nestin, Hes1, and Sox9. (C and D) Expression of acinar cell terminal differentiation markers Mist1, amylase, and elastase return to control levels by 6 weeks after treatment with TM. (E) Amylase and activated CPA (CPA<sup>Active</sup>) protein levels return to control levels over the duration of the time course. S6, loading control; Ctrl, littermate animals treated with corn oil. \**P* < .05.

in 4-week samples, few  $\beta$ -gal-positive cells remained at the later time points, and this decrease correlated with a loss of Xbp1<sup>ΔEx2</sup> transcripts as Xbp1<sup>ΔEx2</sup> acinar cells were replaced by Xbp1<sup>fl/fl</sup> acinar cells (Figure 6C and D and Supplementary Figure 7).

Morphometry analysis of 6- to 8-week post-TM pancreata revealed an almost complete recovery from the Xbp1<sup>ΔEx2</sup> phenotype. The exocrine pancreas consisted predominantly of zymogen-filled acini with little evidence of apoptotic cells (Figure 6E). Although there was a significant increase in adipose tissue, most of the exocrine organ consisted of relatively normal-appearing acinar cells (Figure 6F). However, intermixed with acini were limited areas that retained inflammatory cells, as well as extensive Sox9 positive tubular complexes that were likely derived from the proliferating Hes1/Sox9-positive centroacinar/terminal duct cell population (Figure 6F and Supplementary Figure 8).

Finally, we examined 8- to 12-week Xbp1<sup>ΔEx2</sup> pancreata to determine if regenerated acinar cells resembled age-matched control pancreata. Regenerated acinar cells had well-defined acini that were filled with ZGs (Figure 7A and B). However, individual acinar cells at 8 weeks after treatment with TM were significantly larger than control Xbp1<sup>fl/fl</sup> cells (Figure 7B and C). ZC volumes increased steadily from 2 to 6 weeks

after treatment with TM, after which the regenerating acinar cells were almost 2.5-fold larger than control cells. Interestingly, ZC nuclei also showed an increase in volume, attaining sizes that were 3-fold larger than normal acinar nuclei (Figure 7D). By 12 weeks after treatment with TM, acinar nuclear and cell size remained approximately 2-fold larger than in control littermate samples. These results suggest that regenerated cells exhibited a hypertrophic response, possibly as a resilient mechanism to cope with the extensive cell death associated with Xbp1<sup>ΔEx2</sup> cells.

### Discussion

Understanding the molecular pathways by which cells, tissues, and organs respond and recover from stress is critical to accurately predict and appropriately intercede when aberrant physiologic responses present. Cellular coping mechanisms are often driven by specific responses to a pertinent stressor, including the 3 pathways collectively termed the UPR. The UPR is an important homeostatic mechanism in all cells, but its function is especially important for secretory cells using high-throughput translational machinery. In this study, we conditionally inactivated the Xbp1 locus in adult acinar cells to estab-

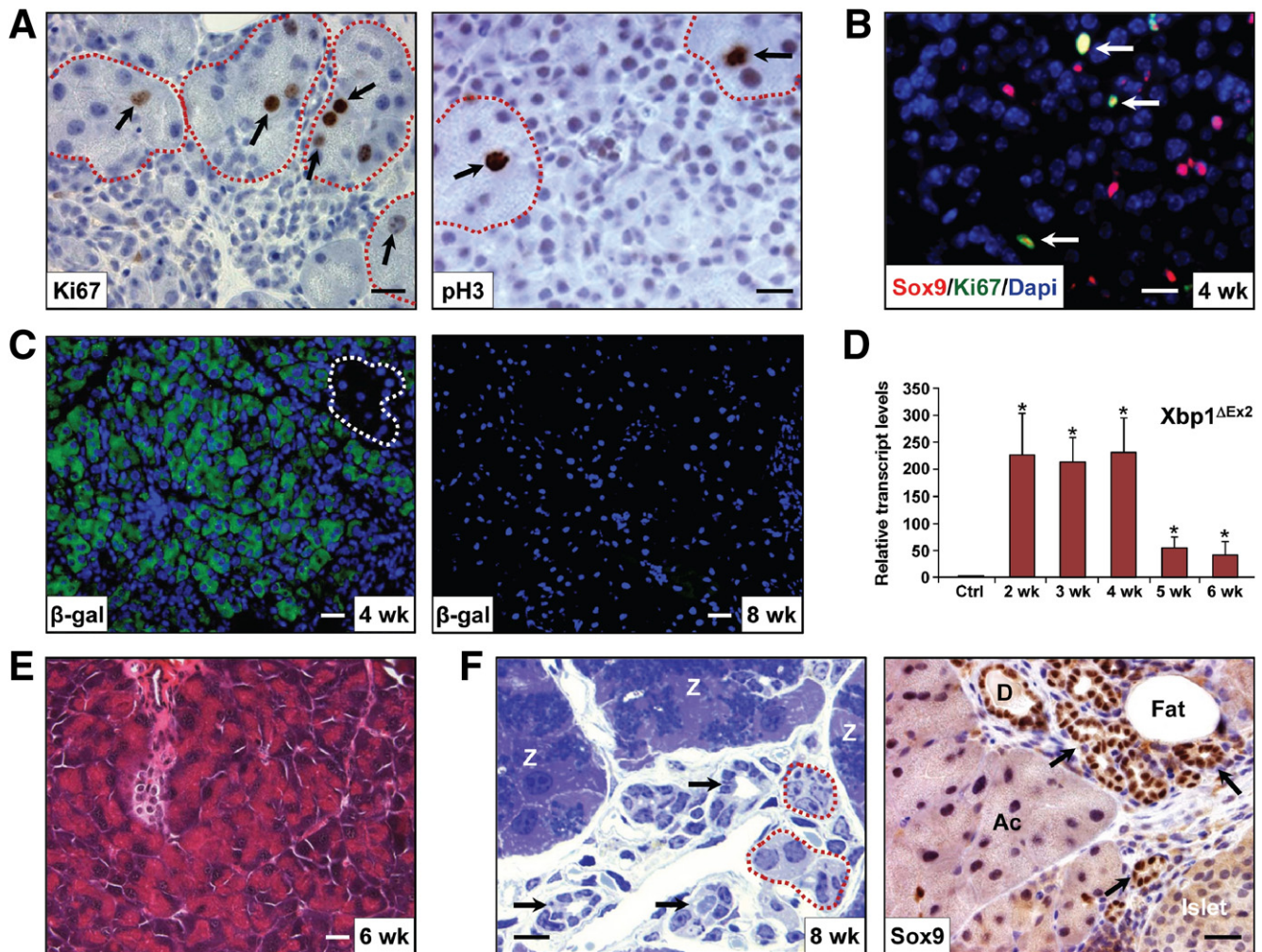


**Figure 6.** The zymogen-containing subset of acinar cells rapidly proliferates and regenerates the exocrine pancreas. (A) Zymogen-containing populations (red outline) are highly proliferative, as evidenced by expression of Ki67 and phospho-histone3 (pH3) (arrows). All nonzymogenic acinar cells remain Ki67 and pH3 negative. (B) The Sox9 centroacinar/terminal duct cell compartment is also highly proliferative. (C) Anti- $\beta$ -gal of 4-week and 8-week  $Xbp1^{\Delta Ex2}$  pancreata showing that the vast majority of acinar cells at 4 weeks after treatment with TM are  $\beta$ -gal positive. By 8 weeks after treatment with TM, the exocrine pancreas consists almost entirely of  $\beta$ -gal-negative acinar cells. The dotted outline highlights a zymogen-containing acinus. (D)  $Xbp1^{\Delta Ex2}$  transcript levels over the indicated time points following addition of TM. As predicted, replacement of  $Xbp1^{\Delta Ex2}$  acinar cells with  $Xbp1^{fl/fl}$  acinar cells leads to a loss of the  $Xbp1^{\Delta Ex2}$  allele. (E) H&E staining reveals the rapid recovery of the acinar cell population by 6 weeks after  $Xbp1$  ablation. (F) Toluidine blue staining of semi-thin sections shows the presence of large numbers of zymogen-containing acini (z) 8 weeks after treatment with TM. ZGs are detected as the dark blue staining in the center of the cells. The recovered pancreas also exhibits several other characteristics, including the presence of tubular duct-like structures (black arrows), occasional nonzymogenic areas (red outlines), and fat deposition. Note that the tubular complexes are Sox9 positive, suggesting that they are derived from the expanding centroacinar/terminal duct cell compartment. D, duct; Ac, acinar cells. Scale bars = 20  $\mu$ m. \* $P < .05$ .

lish the importance of the XBP1 component of the UPR to exocrine pancreas physiology. Our results support a direct and essential role for XBP1 in modulating ER stress events and in maintaining viability of adult acinar cells.

Acinar-specific ablation of  $Xbp1$  triggered a rapid ER stress response within 24 hours, with the PERK, ATF6, and IRE/XBP1 pathways activated but  $Xbp1$ -specific downstream targets uninduced. Despite an otherwise intact UPR,  $Xbp1^{\Delta Ex2}$  adult acinar cells were chronically under ER stress, revealing for the first time that the PERK and ATF6 pathways are insufficient for recovery from ER stress in these cells. The inability of acinar cells to compensate for loss of XBP1 was surprising, given reports that acinar-restricted deletion of PERK failed to produce ER stress.<sup>20</sup> Similarly, germline deletion of  $ATF6\alpha$  resulted in

no cellular or organ defects, although  $ATF6\alpha^{-/-}$  MEFs were more susceptible to chemically induced ER stress.<sup>21</sup> Together, these results support the concept that IRE/XBP1 is the major UPR pathway used by acinar cells to maintain proper ER homeostasis.

Deletion of  $Xbp1$  in a number of specialized secretory cells, including plasma B cells and intestinal Paneth cells, induces significant ER stress and associated alterations in ER architecture.<sup>2,22,23</sup> A similar outcome has recently been observed in stomach ZCs, where deletion of  $Xbp1$  induced ER stress and an altered ER. However, unlike pancreatic acinar cells,  $Xbp1^{\Delta Ex2}$  stomach ZCs survived without this critical regulator, with no evidence of cell loss following  $Xbp1$  deletion.<sup>12</sup> Indeed, stomach ZCs arising after  $Xbp1$  ablation continued to express ZC markers, although defects in the

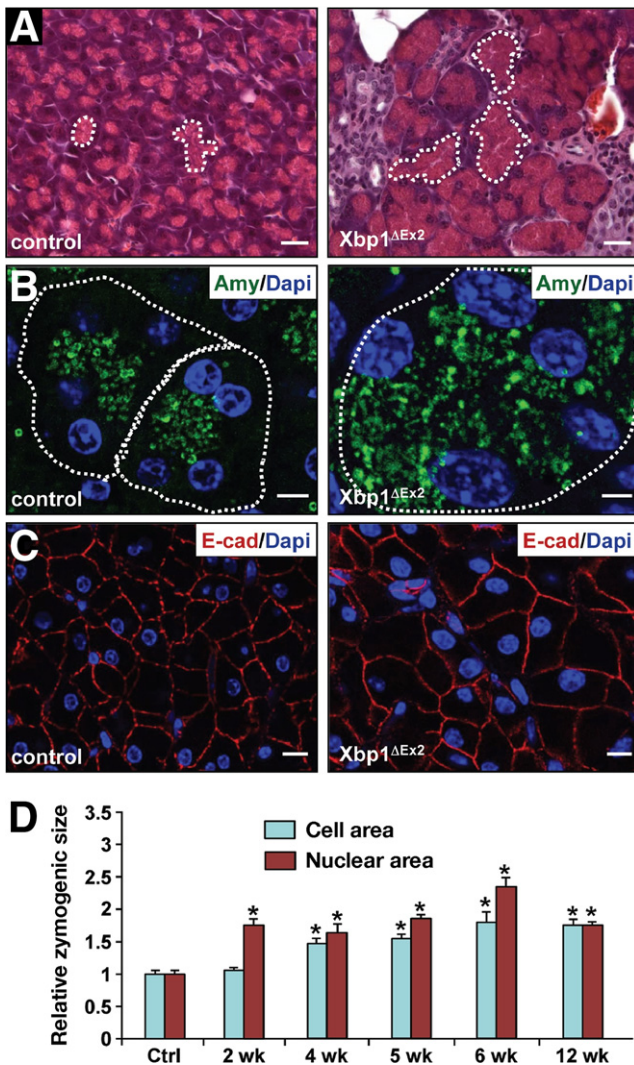


**Figure 7.** Recovered acini have an expanded zymogen compartment and overall increased cell size relative to control pancreata. (A) Comparison between eosin-stained zymogen compartments in control and 12-week postablation pancreata. *White dotted lines* highlight apically localized zymogens from individual acini. (B) Amylase staining in control and 12-week  $Xbp1^{\Delta Ex2}$  pancreata reveal a greatly expanded zymogen compartment in the regenerating acinar cells. *Outlines* indicate individual acini. (C) E-cadherin staining highlights the overall size of individual acinar cells of control and 12-week post-TM pancreata, showing an increased size for the regenerated cells. (D) Quantification of nuclear and acinar cell size for control and  $Xbp1^{\Delta Ex2}$  pancreata. Scale bars = 20  $\mu m$ . \* $P < .005$ .

developmental silencing of progenitor neck cell markers were observed.<sup>12</sup> This is in marked contrast to pancreatic acinar cells, which rapidly lose differentiated cell markers and increase expression of CHOP, a known inducer of apoptosis via repression of Bcl-2. The dramatic difference in cell viability between stomach ZCs and pancreatic acinar cells suggests that the PERK and ATF6 pathways are used to different extents in these functionally related cell types. Additional studies will be required to determine how the distinct arms of the UPR function during development and in mature adult cells within different secretory cell lineages.

Despite extensive cell death throughout the  $Xbp1^{\Delta Ex2}$  exocrine pancreas, isolated areas of zymogen-containing acinar

cells remained, representing the small portion of cells that failed to ablate Xbp1. Interestingly, the escaping  $Xbp1^{\Delta Ex2}$  acinar cells no longer remained quiescent but quickly entered a proliferative phase, a response that is similarly observed in cerulein injury models of regeneration.<sup>24–26</sup> The  $Xbp1^{\Delta Ex2}$  zymogenic acinar cells also retained high levels of MIST1 protein, indicating that these cells failed to completely abrogate their terminal exocrine differentiation program during the proliferative phase. This contrasts with cerulein injury and  $Kras^{G12D}$ -induced acinar-ductal metaplasia, where MIST1 levels are quickly extinguished during the early phases of injury and dedifferentiation.<sup>27</sup> Thus, depending on the initial insult, acinar cells may be capable of using different recovery pathways to regenerate.

In addition to acinar cell regeneration, deletion of Xbp1 in acinar cells also led to proliferation of the centroacinar and terminal duct cell population, distinguishable by expression of the transcription factors Sox9 and Hes1.<sup>16–19</sup> Elegant studies by Rovira et al have shown that this cell population is capable of forming self-renewing pancreatospheres that spontaneously give rise to cells of the endocrine and acinar cell lineages in vitro.<sup>16</sup> This population also becomes greatly expanded in the setting of cerulein-induced pancreatitis,<sup>16</sup> suggesting that a similar regeneration phenomenon occurs on acinar-specific deletion of Xbp1. Although lineage tracing studies cannot be performed on the centroacinar/terminal duct cells in this current  $Xbp1^{\Delta Ex2}$  model, these cells are likely responsible for formation of the Sox9/keratin-19-expressing tubular complexes that form in the recovered pancreas.<sup>18,19</sup> Additional studies will be required to define the fate of the expanded centroacinar cell compartment and to determine if these cells also contribute to other cell lineages on chronic ER stress.

The coordinate pancreatic regeneration observed in this model is accompanied by an acquisition of the normal exocrine pancreas parameters of zymogen production and activation, expression of hallmark transcription factors including Mist1, and a marked reduction in proliferation markers. These changes indicate that the regenerated acinar cells begin to reestablish proper pancreatic function following the elimination of the CHOP-positive, Xbp1-deficient population. Indeed, acini in the recovering organ have a marked increase in cell size, presumably due to compensatory overproduction of zymogens in these acini as the pancreas continues to regenerate. Thus, our study shows that pancreatic renewal can occur, despite a severe ER stress-induced apoptotic event, via proliferation and compensation of the surviving exocrine compartment.

Finally, the regenerative capacity of the adult pancreas in the presence of an ER stress-based alteration provides a unique opportunity to exploit UPR pathways for therapeutic purposes. Studies using modification of the UPR to compromise transformed cell growth have shown promise in cancer cell lines<sup>28</sup> and in murine models of tumor development,<sup>29</sup> and several studies have shown efficacy of bortezomib in sensitizing pancreatic cancer cells to ER stress-induced apoptosis.<sup>30–32</sup> Future approaches should focus on (1) developing new cell-targeted strategies to

inhibit XBP1 function in pancreatic tumors and (2) increasing the regenerative response of the remaining non-transformed cells of the exocrine pancreas.

### Supplementary Material

Note: To access the supplementary material accompanying this article, visit the online version of *Gastroenterology* at [www.gastrojournal.org](http://www.gastrojournal.org) and at doi: [10.1053/j.gastro.2011.06.045](https://doi.org/10.1053/j.gastro.2011.06.045).

### References

- Williams JA. Regulation of acinar cell function in the pancreas. *Curr Opin Gastroenterol* 2010;26:478–483.
- Todd DJ, McHeyzer-Williams LJ, Kowal C, et al. XBP1 governs late events in plasma cell differentiation and is not required for antigen-specific memory B cell development. *J Exp Med* 2009;206:2151–2159.
- Lee AH, Chu GC, Iwakoshi NN, et al. XBP-1 is required for biogenesis of cellular secretory machinery of exocrine glands. *EMBO J* 2005;24:4368–4380.
- Lee AH, Scapa EF, Cohen DE, et al. Regulation of hepatic lipogenesis by the transcription factor XBP1. *Science* 2008;320:1492–1496.
- Back SH, Scheuner D, Han J, et al. Translation attenuation through eIF2alpha phosphorylation prevents oxidative stress and maintains the differentiated state in beta cells. *Cell Metab* 2009;10:13–26.
- Kowalik AS, Johnson CL, Chadi SA, et al. Mice lacking the transcription factor Mist1 exhibit an altered stress response and increased sensitivity to caerulein-induced pancreatitis. *Am J Physiol Gastrointest Liver Physiol* 2007;292:G1123–G1132.
- Kubisch CH, Logsdon CD. Secretagogues differentially activate endoplasmic reticulum stress responses in pancreatic acinar cells. *Am J Physiol Gastrointest Liver Physiol* 2007;292:G1804–G1812.
- Ron D, Walter P. Signal integration in the endoplasmic reticulum unfolded protein response. *Nat Rev Mol Cell Biol* 2007;8:519–529.
- Kubisch CH, Logsdon CD. Endoplasmic reticulum stress and the pancreatic acinar cell. *Expert Rev Gastroenterol Hepatol* 2008;2:249–260.
- Kubisch CH, Sans MD, Arumugam T, et al. Early activation of endoplasmic reticulum stress is associated with arginine-induced acute pancreatitis. *Am J Physiol Gastrointest Liver Physiol* 2006;291:G238–G245.
- Romero-Ramirez L, Cao H, Regalado MP, et al. X box-binding protein 1 regulates angiogenesis in human pancreatic adenocarcinomas. *Transl Oncol* 2009;2:31–38.
- Huh WJ, Esen E, Geahlen JH, et al. XBP1 controls maturation of gastric zymogenic cells by induction of MIST1 and expansion of the rough endoplasmic reticulum. *Gastroenterology* 2010;139:2038–2049.
- Habbe N, Shi G, Meguid RA, et al. Spontaneous induction of murine pancreatic intraepithelial neoplasia (mPanIN) by acinar cell targeting of oncogenic Kras in adult mice. *Proc Natl Acad Sci U S A* 2008;105:18913–18918.
- Shi G, Zhu L, Sun Y, et al. Loss of the acinar-restricted transcription factor Mist1 accelerates Kras-induced pancreatic intraepithelial neoplasia. *Gastroenterology* 2009;136:1368–1378.
- Pin CL, Rukstalis JM, Johnson C, et al. The bHLH transcription factor Mist1 is required to maintain exocrine pancreas cell organization and acinar cell identity. *J Cell Biol* 2001;155:519–530.
- Rovira M, Scott SG, Liss AS, et al. Isolation and characterization of centroacinar/terminal ductal progenitor cells in adult mouse pancreas. *Proc Natl Acad Sci U S A* 2010;107:75–80.
- Seymour PA, Freude KK, Tran MN, et al. SOX9 is required for maintenance of the pancreatic progenitor cell pool. *Proc Natl Acad Sci U S A* 2007;104:1865–1870.
- Furuyama K, Kawaguchi Y, Akiyama H, et al. Continuous cell supply from a Sox9-expressing progenitor zone in adult liver, exocrine pancreas and intestine. *Nat Genet* 2011;43:34–41.
- Kopinke D, Brailsford M, Shea JE, et al. Lineage tracing reveals the dynamic contribution of Hes1+ cells to the developing and adult pancreas. *Development* 2011;138:431–441.
- Iida K, Li Y, McGrath BC, et al. PERK eIF2 alpha kinase is required to regulate the viability of the exocrine pancreas in mice. *BMC Cell Biol* 2007;8:38.
- Wu J, Rutkowski DT, Dubois M, et al. ATF6alpha optimizes long-term endoplasmic reticulum function to protect cells from chronic stress. *Dev Cell* 2007;13:351–364.
- Reimold AM, Iwakoshi NN, Manis J, et al. Plasma cell differentiation requires the transcription factor XBP-1. *Nature* 2001;412:300–307.
- Kaser A, Lee AH, Franke A, et al. XBP1 Links ER stress to intestinal inflammation and confers genetic risk for human inflammatory bowel disease. *Cell* 2008;134:743–756.
- Desai BM, Oliver-Krasinski J, De Leon DD, et al. Preexisting pancreatic acinar cells contribute to acinar cell, but not islet beta cell, regeneration. *J Clin Invest* 2007;117:971–977.
- Fendrich V, Esni F, Garay MV, et al. Hedgehog signaling is required for effective regeneration of exocrine pancreas. *Gastroenterology* 2008;135:621–631.
- Strobel O, Dor Y, Alsina J, et al. In vivo lineage tracing defines the role of acinar-to-ductal transdifferentiation in inflammatory ductal metaplasia. *Gastroenterology* 2007;133:1999–2009.
- Jensen JN, Cameron E, Garay MV, et al. Recapitulation of elements of embryonic development in adult mouse pancreatic regeneration. *Gastroenterology* 2005;128:728–741.
- Romero-Ramirez L, Cao H, Nelson D, et al. XBP1 is essential for survival under hypoxic conditions and is required for tumor growth. *Cancer Res* 2004;64:5943–5947.
- Bobrovnikova-Marjon E, Grigoriadou C, Pytel D, et al. PERK promotes cancer cell proliferation and tumor growth by limiting oxidative DNA damage. *Oncogene* 2010;29:3881–3895.
- Nawrocki ST, Carew JS, Dunner K Jr, et al. Bortezomib inhibits PKR-like endoplasmic reticulum (ER) kinase and induces apoptosis via ER stress in human pancreatic cancer cells. *Cancer Res* 2005;65:11510–11519.
- Nawrocki ST, Carew JS, Pino MS, et al. Aggresome disruption: a novel strategy to enhance bortezomib-induced apoptosis in pancreatic cancer cells. *Cancer Res* 2006;66:3773–3781.
- Nawrocki ST, Carew JS, Pino MS, et al. Bortezomib sensitizes pancreatic cancer cells to endoplasmic reticulum stress-mediated apoptosis. *Cancer Res* 2005;65:11658–11666.

Received December 5, 2010. Accepted June 13, 2011.

#### Reprint requests

Address requests for reprints to: Stephen F. Konieczny, PhD, Department of Biological Sciences and the Purdue Center for Cancer Research, Purdue University, Hansen Life Sciences Research Building, 201 South University Street, West Lafayette, Indiana 47907-2064. e-mail: [sfk@purdue.edu](mailto:sfk@purdue.edu).

#### Acknowledgments

D.A.H. and S.E.H. contributed equally to this work. The authors thank Dr Michael Logan for providing histopathologic analysis, David Miley for generating histology slides, and Patrick Schweickert for quantitative analysis.

#### Conflicts of interest

The authors disclose no conflicts.

#### Funding

Supported by National Institutes of Health grants DK55489 and CA124586 (to S.F.K.), National Institutes of Health grant AI32412 (to L.H.G.), and AHA grant 0835610P (to A.-H.L.).